Two-dimensional stimulated Raman scattering of short laser pulses

C. J. McKinstrie,[1,3] R. Betti,[1,3] R. E. Giacone,[1,3] T. Kolber,[1,3] and E. J. Turano[2,3]
[1]*Department of Mechanical Engineering, University of Rochester, Rochester, New York 14627*
[2]*Department of Physics and Astronomy, University of Rochester, Rochester, New York 14627*
[3]*Laboratory for Laser Energetics, 250 East River Road, Rochester, New York 14623*
(Received 12 August 1994)

The evolution of the stimulated Raman scattering (SRS) instability in time and two spatial dimensions is studied analytically for initial and boundary conditions representative of a laser pulse convecting into fresh plasma. For most scattering angles, SRS saturates due to the lateral convection of the Stokes wave. The steady-state amplitude profiles of the Stokes and Langmuir waves are highly two dimensional.

PACS number(s): 52.35.Mw, 52.35.Nx, 52.40.Nk, 42.65.Dr

Simulated Raman scattering (SRS) is the decay of an incident light wave (0) into a frequency-downshifted, or Stokes, light wave (1) and a Langmuir wave (2). The conservation of energy and momentum is reflected in the frequency and wave-vector matching conditions

$$\omega_0=\omega_1+\omega_2\ ,\quad \mathbf{k}_0=\mathbf{k}_1+\mathbf{k}_2\ , \tag{1}$$

the second of which is illustrated in Fig. 1. Recently, there has been a resurgence of interest in the spatiotemporal evolution of parametric instabilities such as SRS and stimulated Brillouin scattering (SBS) [1–5], driven by the realization that the transient phase of these instabilities dominates many current experiments. In experiments relevant to inertial confinement fusion, SBS fails to reach steady state because of the intrinsic slowness of the ion-acoustic wave, which limits how quickly transients convect out of the interaction region. In experiments relevant to plasma accelerators and light sources, transient SRS is important because of the intrinsic shortness of the high-intensity laser pulses.

In the weak-coupling regime, the initial evolution of SRS in homogeneous plasma is governed by the linearized equations

$$\begin{aligned}&(\partial_t+v_{1x}\partial_x+v_{1y}\partial_y)A_1=\gamma_0 A_2\ ,\\&(\partial_t+v_{2x}\partial_x)A_2=\gamma_0 A_1\ ,\end{aligned} \tag{2}$$

where A_1 represents the vector potential associated with the Stokes wave, A_2 represents the plasma density fluctuation associated with the Langmuir wave, and $\gamma_0=\omega_2 c|\mathbf{k}_2|A_0/4[\omega_2(\omega_0-\omega_2)]^{1/2}$ is the temporal growth rate of SRS in an infinite plasma [6]. It is convenient to measure distance (x) backward from the leading edge of the laser pulse, as shown in Fig. 2. With this convention the "pulse-frame" group velocities are given, in the cold-plasma approximation, by $\mathbf{v}_1=(c-c\cos\theta, c\sin\theta)$ and $\mathbf{v}_2=(c,0)$, where θ is the laboratory-frame scattering angle. The analysis of SRS divides naturally into two cases: forward SRS, in which $v_{1x}<v_{2x}$, and sideward and backward SRS, in which $v_{1x}\geq v_{2x}$.

For forward SRS the solution of Eqs. (2), in the domain illustrated in Fig. 3(a), is facilitated by the change of variables $x'=x$, $y'=v_{1x}y/v_{1y}$, $t'=v_{1x}(v_{2x}t-x)/(v_{2x}-v_{1x})$, $B_1=v_{1x}^{1/2}A_1$, and $B_2=v_{2x}^{1/2}A_2$. Physically, t' is the retarded time, measured from the arrival of the faster wave, and B_1 and B_2 are proportional to the action flux amplitudes of the Stokes and Langmuir waves, respectively. Using the new variables, Eqs. (2) can be rewritten as

$$(\partial_{t'}+\partial_{x'}+\partial_{y'})B_1=\gamma B_2,\quad \partial_{x'}B_2=\gamma B_1\ . \tag{3}$$

These equations are to be solved in the domain $\{(t',x',y'):\ t'\geq 0,\ x'\geq 0,\ \text{and}\ y'\geq 0\}$, which is illustrated in Fig. 3(b), subject to the initial conditions

$$B_1(0,x',y')=0,\quad B_2(0,x',y')=1 \tag{4}$$

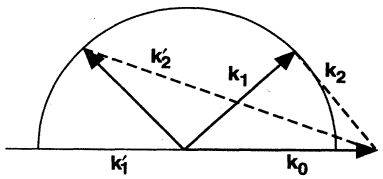

FIG. 1. Geometry of SRS in the laboratory frame. The Langmuir frequency ω_2 is equal to the electron plasma frequency, $k_1=[(\omega_0-\omega_2)^2-\omega_2^2]^{1/2}/c$, $\mathbf{k}_1=(k_1\cos\theta,k_1\sin\theta)$, and $\mathbf{k}_2=(k_0-k_1\cos\theta,-k_1\sin\theta)$.

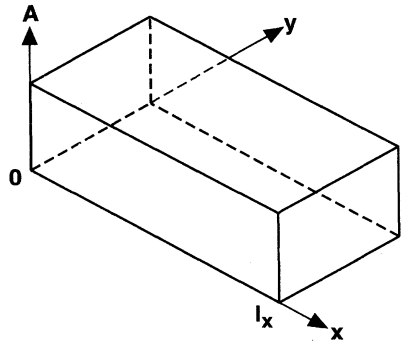

FIG. 2. Snapshot of the laser pulse. The front boundary of the interaction region is defined by the leading edge of the laser pulse and is located at $x=0$. For $t\leq l_x/c$ the rear boundary of the interaction region is defined by the plasma boundary and is located at $x=ct$. For $t>l_x/c$ it is defined by the trailing edge of the laser pulse and is located at $x=l_x$.

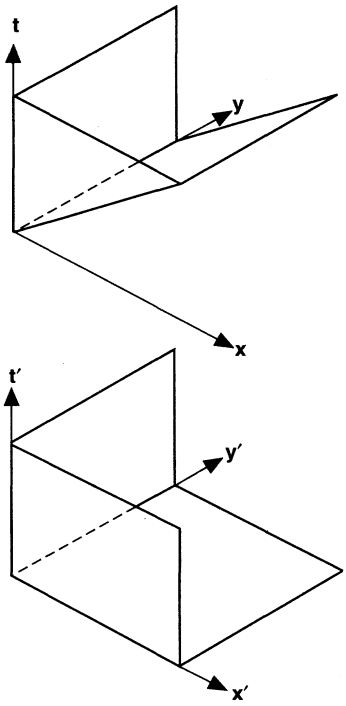

FIG. 3. Domain of interest illustrated in (a) the original pulse-frame coordinates and (b) the characteristic coordinates defined in the text preceding Eqs. (3).

and the boundary conditions

$$B_1(t',0,y')=0, \quad B_2(t',0,y')=1 ,$$
$$B_1(t',x',0)=0, \quad B_2(t',x',0)=1 . \tag{5}$$

These conditions are representative of a laser pulse convecting into fresh plasma, in which a constant level of Langmuir fluctuations is available to seed the instability. They allow the instability to proceed from the moment the leading edge of the laser pulse enters the plasma. for future reference, we comment that the initial conditions of Mori *et al.* [3] do not allow the instability to proceed until the entire laser pulse has entered the plasma.

Equations (3)–(5) are similar in form to the SBS equations solved by McKinstrie *et al.* [4]. It follows immediately that

$$B_j(t',x',y')=B_j(t',x')H(y'-t')+t'\leftrightarrow y' , \tag{6}$$

where $B_1(t',x')$ and $B_2(t',x')$ are the solutions of the one-dimensional (1D) limit of Eqs. (3), in which the y' derivative term is omitted, and H is the Heaviside step function. Far from the boundary at $y'=0$, the waves evolve in x' and t'. When $t'=y'$, the information that a side boundary exists reaches the waves, which stop growing immediately if they have not already done so.

It is not difficult to solve the 1D equations using Laplace transforms. The result is

$$B_1(t',x')=\begin{cases}\displaystyle\sum_{n=0}^{\infty}[t'/(x'-t')]^{n+1/2}I_{2n+1} \\ \quad\times(2\gamma[t'(x-t')]^{1/2}), \quad t'<x' \\ \sinh(\gamma x') , \quad t'\geq x' ,\end{cases}$$
$$B_2(t',x')=\begin{cases}\displaystyle\sum_{n=0}^{\infty}[t'/(x'-t')]^{n}I_{2n} \\ \quad\times(2\gamma[t'(x'-t')]^{1/2}), \quad t'<x' \\ \cosh(\gamma x') , \quad t'\geq x',\end{cases} \tag{7}$$

where I_n is the modified Bessel function of the first kind, of order n.

Taken together, Eqs. (6) and (7) describe the solution of Eqs. (3)–(5). The $x'y'$ plane is divided into three regions, in which SRS is characterized by 1D spatiotemporal growth [the first form of Eqs. (7)], 2D spatial growth [the first form of Eqs. (7) with $t'\leftrightarrow y'$], and 1D spatial growth [the second form of Eqs. (7)], as illustrated in Fig. 4(a).

In terms of the original independent variables, the solution can be rewritten as

$$B_1(t,x)=\begin{cases}\displaystyle\sum_{n=0}^{\infty}\left[\frac{v_{1x}}{v_{2x}}\right]^{n+1/2}\left[\frac{v_{2x}t-x}{x-v_{1x}t}\right]^{n+1/2}I_{2n+1}\left[\frac{2\gamma_0[(v_{2x}t-x)(x-v_{1x}t)]^{1/2}}{v_{2x}-v_{1x}}\right] , \\ \displaystyle\sum_{n=0}^{\infty}\left[\frac{v_{1x}y}{v_{1y}x-v_{1x}y}\right]^{n+1/2}I_{2n+1}\left[\frac{2\gamma_0[v_{1x}y(v_{1y}x-v_{1x}y)]^{1/2}}{v_{1y}(v_{1x}v_{2x})^{1/2}}\right] , \\ \sinh[\gamma_0 x/(v_{1x}v_{2x})^{1/2}] ,\end{cases}$$
$$B_2(t,x)=\begin{cases}\displaystyle\sum_{n=0}^{\infty}\left[\frac{v_{1x}}{v_{2x}}\right]^{n}\left[\frac{v_{2x}t-x}{x-v_{1x}t}\right]^{n}I_{2n}\left[\frac{2\gamma_0[(v_{2x}t-x)(x-v_{1x}t)]^{1/2}}{v_{2x}-v_{1x}}\right] , \\ \displaystyle\sum_{n=0}^{\infty}\left[\frac{v_{1x}y}{v_{1y}x-v_{1x}y}\right]^{n}I_{2n}\left[\frac{2\gamma_0[v_{1x}y(v_{1y}x-v_{1x}y)]^{1/2}}{v_{1y}(v_{1x}v_{2x})^{1/2}}\right] , \\ \cosh[\gamma_0 x/(v_{1x}v_{2x})^{1/2}] ,\end{cases} \tag{8}$$

where the first form is valid in region I [$v_{1x}t<x\leq v_{2x}t$ and $y\geq v_{1y}(v_{2x}t-x)/(v_{2x}-v_{1x})$], the second form is valid in region II [$x<v_{2x}t$, and $y<v_{1y}x/v_{1x}$ and $v_{1y}(v_{2x}t-x)/(v_{2x}-v_{1x})$], and the third form is valid in region III [$x\leq v_{1x}t$

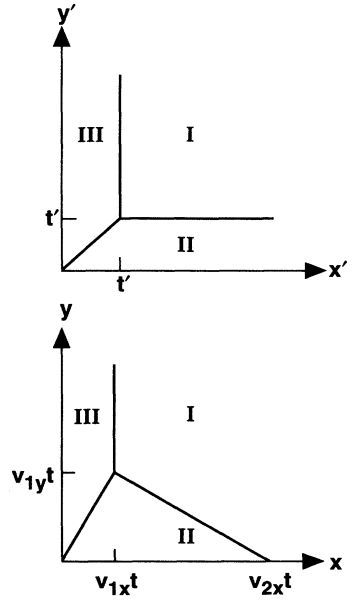

FIG. 4. Solution regions in (a) characteristic and (b) pulse-frame coordinates. SRS is characterized by 1D spatiotemporal growth in region I, 2D spatial growth in region II, and 1D spatial growth in region III.

and $y \geq v_{1y}x/v_{1x}$]. These regions are illustrated in Fig. 4(b). Solution (8) was derived under the assumption that the laser pulse length is infinite. However, SRS is a convective instability in the pulse frame and there are no additional boundary conditions to be satisfied by the Stokes and Langmuir waves as they pass through the rear and side boundaries of the laser pulse. Thus, solution (8) also describes the evolution of SRS within a finite laser pulse.

For a scattering angle of 0°, corresponding to directly forward SRS, $\mathbf{v}_1=\mathbf{0}$. Solution (8) is well defined in the limit that $\mathbf{v}_1 \to \mathbf{0}$ and reduces to

$$A_1(t,x,y)=[(v_{2x}t-x)/x]^{1/2} \times I_1(2\gamma_0[(v_{2x}t-x)x]^{1/2}/v_{2x}) ,$$
$$A_2(t,x,y)=I_0(2\gamma_0[(v_{2x}t-x)x]^{1/2}/v_{2x}) . \quad (9)$$

Solution (9) is written in terms of the original wave amplitudes because it is not meaningful to consider the action flux amplitudes when $\mathbf{v}_1=\mathbf{0}$. (The main effect of the anti-Stokes light wave, which cannot be neglected when $\theta \approx 0°$, is to renormalized γ_0 [6].) At any point (x,y) in the pulse frame, there is no growth until the plasma boundary reaches that point at $t=x/v_{2x}$. For $t>x/v_{2x}$ the point lies within the plasma and it is meaningful to consider the evolution of SRS at that point. The growth of SRS is spatiotemporal in nature throughout the entire interaction region. This result differs from the result of Mori *et al.* [3] in that there is no region in which the growth of SRS is temporal. This difference is due to the different initial conditions that were imposed, as we mentioned earlier.

Snapshots of the Langmuir amplitude at two different times are displayed in Figs. 5 and 6 for a scattering angle of 45°. Three distinct regions of growth can be seen in each figure, as described in the text following Eqs. (8). For $t>x/v_{2x}$, the wave amplitudes grow nonexponentially in time according to the first form of Eqs. (8). However, in contrast to the case described in the preceding paragraph, SRS eventually saturates. For $y \geq v_{1y}x/v_{1x}$, the evolution of SRS is one dimensional: SRS saturates due to the convection of the Stokes wave in the x direction, in a time

$$t_{1D}=x/v_{1x} . \quad (10)$$

For $y<v_{1y}x/v_{1x}$, the evolution of SRS is two dimensional: SRS saturates due to the convection of the Stokes wave in the y direction in a time

$$t_{2D}=\frac{x}{v_{2x}}+\frac{(v_{2x}-v_{1x})y}{v_{2x}v_{1y}} . \quad (11)$$

Equation (11) generalizes the result that $t_{2D} \approx y/v_{1y}$ when $v_{1x} \ll v_{2x}$ and $v_{1y} \ll v_{2x}$ [4]. In steady state the Langmuir wave attains its peak amplitude at the point (l_x,l_y). Since $t_{2D}<t_{1D}$ at this point, the peak Langmuir amplitude is less than that predicted by a 1D analysis.

In the preceding paragraph it was shown that x/v_{1x} is an upper bound on the saturation time of forward SRS. This result reflects the fact that the convection of transients out of the interaction region is limited by the slower of the Stokes and Langmuir waves. As $\theta \to 90°$, $v_{1x} \to v_{2x}$ and the saturation time of SRS coincides with the arrival time of the plasma boundary: the region of

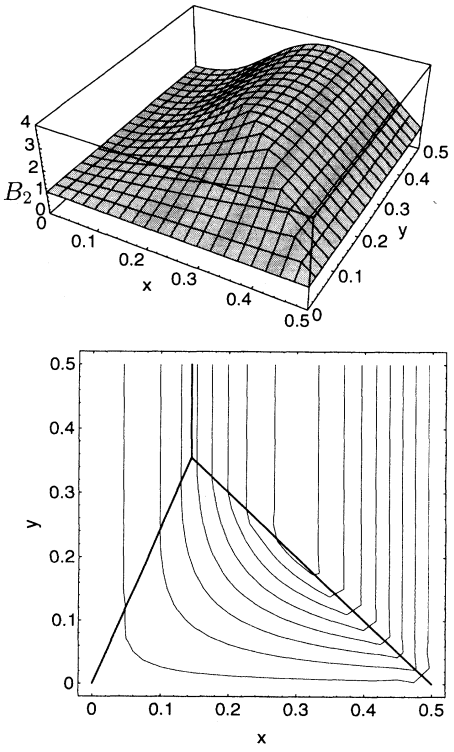

FIG. 5. Snapshot of the Langmuir amplitude B_2, obtained from Eqs. (8), for a scattering angle of 45°. Distance is measured in units of the laser pulse length l_x, the laser aspect ratio $l_y/l_x=0.5$, the laser strength parameter $\gamma_0 l_x/v_{2x}=5$, and the time parameter $v_{2x}t/l_x=0.5$.

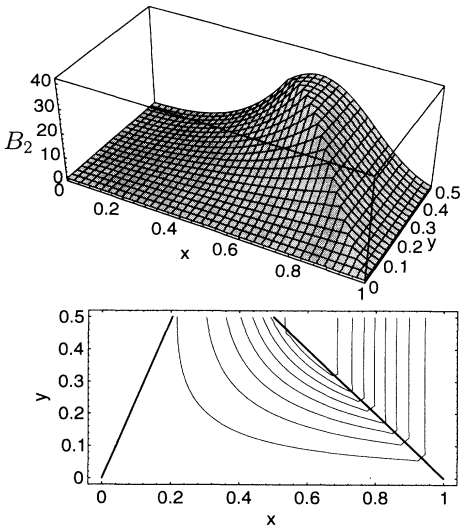

FIG. 6. Snapshot of the Langmuir amplitude B_2, obtained from Eqs. (8), for a scattering angle of 45°. The time parameter $v_{2x}t/l_x = 1.0$ and the other parameters are the same as those associated with Fig. 5.

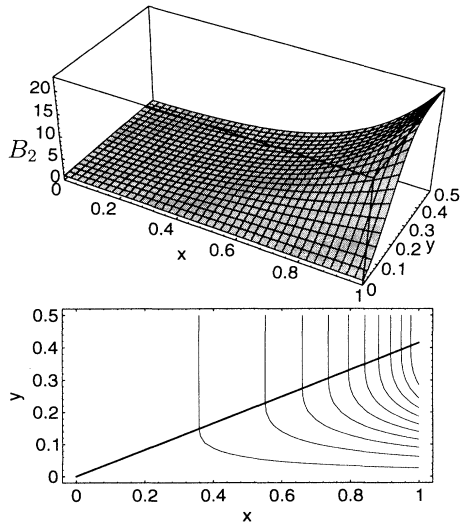

FIG. 7. Snapshot of the Langmuir amplitude B_2, obtained from the second and third forms of Eqs. (8), for a scattering angle of 135°. The parameters are the same as those associated with Fig. 6.

spatiotemporal growth does not exist and SRS is in steady state throughout the entire interaction region. This statement must also be true of backward SRS, for which $v_{1x} > v_{2x}$. Furthermore, in steady state there is no need to distinguish between the fast and slow waves, so the second and third forms of solution (8) must also apply to backward SRS. Both of these assertions can be verified by a formal analysis based on the method of characteristics.

A snapshot of the Langmuir amplitude is displayed in Fig. 7 for a scattering angle of 135°. Because the laser pulse has an aspect ratio $l_y/l_x = 0.5$, the evolution of a significant portion of the Langmuir wave is one dimensional. However, typical aspect ratios are much smaller than unity and the evolution of the Langmuir wave is predominantly two dimensional. The Langmuir wave attains its peak amplitude at the point (l_x, l_y).

The preceding analysis shows that at no time, and for no scattering angle, does the Langmuir amplitude $A_2(t, l_x, l_y)$ grow exponentially in time with growth rate γ_0. Furthermore, for most scattering angles the saturation time (11) is not equal to the time taken by the Stokes wave to cross the interaction region in the y direction. Thus, one cannot estimate the peak Langmuir amplitude accurately by using the traditional formula $\exp(\gamma_0 l_y/v_{1y})$. Even in steady state, the amplification of the Langmuir wave is a 2D process and the peak Langmuir amplitude cannot be predicted by a model based on the assumption of 1D growth in a judiciously chosen direction. The main defect of the cold-plasma approximation is that it prevents the Langmuir wave from convecting in the y direction as it does in a warm plasma. This shortcoming limits the applicability of solution (8) to laser pulses with aspect ratios $l_y/l_x > v_{2y}/v_{2x}$. This condition is satisfied in current experiments with short laser pulses [7].

We plan to use our results to improve a previous study of the angular dependence of SRS in experiments with short laser pulses [8] and to extend our analysis to include realistic Langmuir noise sources [1,2] and laser pulses of arbitrary intensity [3]. Our results also make possible a comparison of SRS and other 2D processes, such as self-focusing [9], self-modulation [10], and laser hosing [11].

This work was supported by the National Science Foundation under Contract No. PHY-9057093, the U.S. Department of Energy Office of Inertial Confinement Fusion under Cooperative Agreement No. DE-FC03-92SF19460, the University of Rochester, and the New York State Energy Research and Development Authority.

[1] E. A. Williams and R. R. McGowan, in *Research Trends in Physics: Inertial Confinement Fusion,* edited by K. A. Brueckner (AIP, New York, 1992), p. 325.
[2] P. Mounaix, D. Pesme, W. Rozmus, and M. Casanova, Phys. Fluids B **5**, 3304 (1993).
[3] W. B. Mori, C. D. Decker, D. E. Hinkel, and T. Katsouleas, Phys. Rev. Lett. **72**, 1482 (1994).
[4] C. J. McKinstrie, R. Betti, R. E. Giacone, T. Kolber, and J. S. Li, Phys. Rev. E **50**, 2182 (1994).
[5] D. E. Hinkel, E. A. Williams, and R. L. Berger, Phys. Plasmas **1**, 2987 (1994).
[6] W. L. Kruer, *The Physics of Laser Plasma Interactions* (Addison-Wesley, Redwood City, CA, 1988), Chap. 7.
[7] C. B. Darrow, C. Coverdale, M. D. Perry, W. B. Mori, C. Clayton, K. Marsh, and C. Joshi, Phys. Rev. Lett. **69**, 442 (1992).
[8] C. J. McKinstrie and R. Bingham, Phys. Fluids B **4**, 2626 (1992).
[9] T. M. Antonsen, Jr. and P. Mora, Phys. Rev. Lett. **69**, 2204 (1992).
[10] E. Esarey, J. Krall, and P. Sprangle, Phys. Rev. Lett. **72**, 2887 (1994).
[11] J. S. Wurtele and G. Shvets, Bull. Am. Phys. Soc. **38**, 1998 (1993).

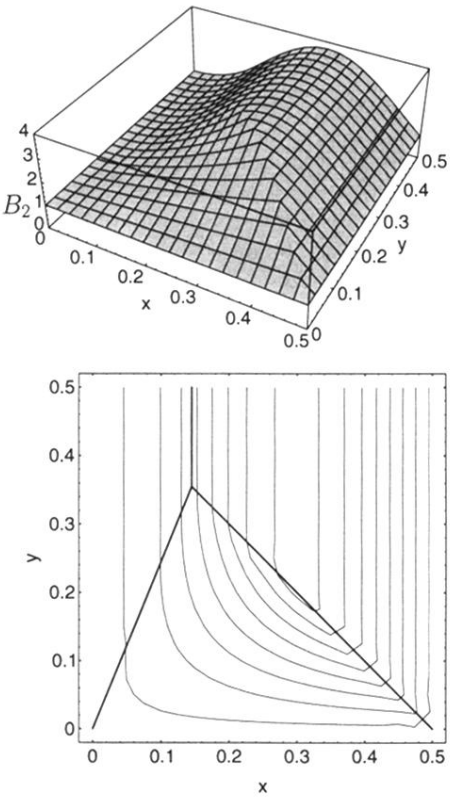

FIG. 5. Snapshot of the Langmuir amplitude B_2, obtained from Eqs. (8), for a scattering angle of 45°. Distance is measured in units of the laser pulse length l_x, the laser aspect ratio $l_y/l_x=0.5$, the laser strength parameter $\gamma_0 l_x/v_{2x}=5$, and the time parameter $v_{2x}t/l_x=0.5$.

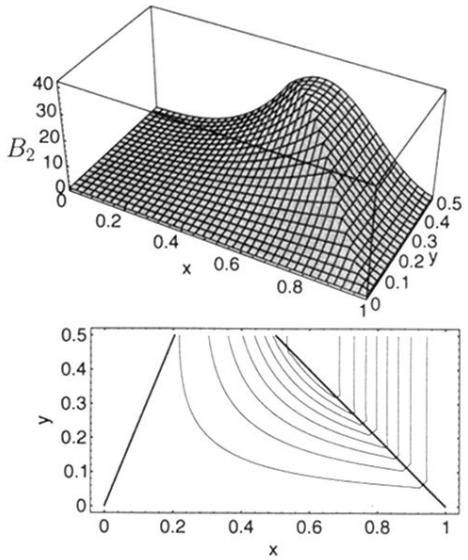

FIG. 6. Snapshot of the Langmuir amplitude B_2, obtained from Eqs. (8), for a scattering angle of 45°. The time parameter $v_{2x}t/l_x = 1.0$ and the other parameters are the same as those associated with Fig. 5.

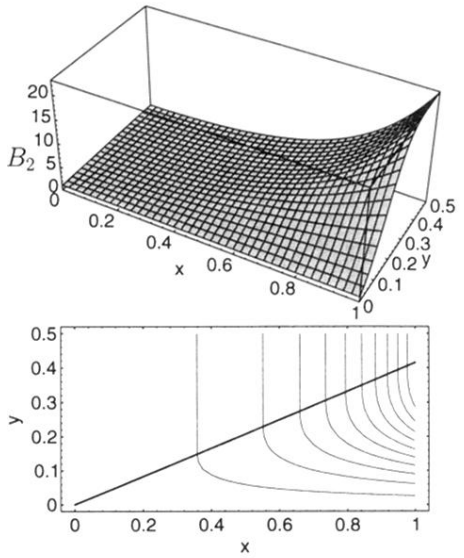

FIG. 7. Snapshot of the Langmuir amplitude B_2, obtained from the second and third forms of Eqs. (8), for a scattering angle of 135°. The parameters are the same as those associated with Fig. 6.